Gas-Phase Backmixing in Bubble-Column Reactors

S. A. Shetty and M. V. Kantak
Chemical Engineering Dept., University of Tulsa, Tulsa, OK 74104

B. G. Kelkar
Petroleum Engineering Dept., University of Tulsa, Tulsa, OK 74104

Gas-phase backmixing and holdup for the air-water system were measured in 0.15- and 0.25-m-dia. bubble columns. Novel experimental and analytical techniques were used to analyze the gas-phase residence time distribution. A Levenberg-Marquardt-type optimization scheme was used to obtain the two reactor model parameters: Peclet and Stanton numbers. Operating variables included the column diameter and the superficial gas- and liquid-phase velocities.

A two-bubble-class hydrodynamic model has been proposed to predict the gas-phase backmixing in bubble column reactors. The model assumes a bimodal distribution of the gas phase with large bubbles flowing in a plug-flow manner and the small bubbles partially backmixed. The model only needs easily measurable parameters and has been validated by comparing experimental as well as literature data on gas-phase backmixing with the model predictions. The model is more realistic than the conventional single-bubble-class model and provides a rational approach to predict the gas-phase backmixing in scaling-up bubble-column reactors.

Introduction

Gas-liquid reactions are of considerable importance in the chemical industry. Typical processes include oxidation, hydrogenation, chlorination, sulphonation, and gas purification by scrubbing. Though it is often possible to carry out many of these reactions in the gas phase, economic and other reasons favor a gas-liquid operation. In petrochemical applications, bubble-column reactors are advantageous over fixed-bed reactors due to improved selectivity resulting from excellent temperature control. The increasing use of bubble columns in the fields of biotechnology and waste water treatment can also be noted. Vertically sparged bubble columns are frequently used in various chemical processes including coal liquefaction, fermentation, Fischer-Tropsch synthesis, and production of liquid fuels from biological materials.

A simple, but very effective, contacting system for gas-liquid reaction is provided by bubble-column reactors for large interfacial area and strong turbulence at the interface. Bubble columns are contactors of simple construction in which a gas or a mixture of gases is distributed at the base by a suitable distributor and moves in the form of a dispersed phase of bubbles relative to a continuous phase. The continuous phase can be a liquid or a homogeneous slurry of reactive or catalytic solids. The columns may be operated in a semibatch, countercurrent or cocurrent manner.

Dimensioning and scale-up of bubble column reactors can be very difficult, despite their simple construction due to the complex interrelations among the many parameters that determine the behavior of bubble columns. Gas-phase backmixing is one of the important hydrodynamic parameters to be considered in the scale-up of bubble columns. It can adversely affect the reaction rates and product selectivity. The mechanism of mixing in the gas phase in the homogeneous regime differs distinctly from that in the heterogeneous regime. In the homogeneous regime, uniform sized bubbles rise in the quiescent liquid without hindering each other. At higher gas velocities, the flow becomes chaotic and is characterized by fast moving large bubbles in the presence of small bubbles. This is the heterogeneous or churn-turbulent regime; however, only unified empirical correlations exist in literature to predict the gas-phase dispersion coefficient. Available data on gas-phase backmixing also reveal considerable scatter among various cor-

---

Correspondence concerning this article should be addressed to B. G. Kelkar.

relations. A more fundamental approach based on theoretical concepts, rather than empirical relationships, is needed to model the gas-phase backmixing in bubble columns.

The present investigation focuses on the measurement of the gas-phase dispersion along with gas holdup and volumetric mass-transfer coefficient in tall bubble columns with cocurrent flow of the phases. A two-bubble-class hydrodynamic model has been proposed to predict the gas-phase backmixing in bubble columns. It is observed that at high gas velocities, typically above the gas transition velocity at which the flow changes from the homogeneous to churn-turbulent regime, the homogeneous gas-in-liquid system cannot be maintained and two bubble classes develop. Large bubbles are assumed to travel in a plug-flow manner due to their high rise velocities, and small bubbles, which are carried with the recirculated liquid, are assumed to be backmixed with a dispersion coefficient equal to that of the liquid phase. Each bubble class contributes to the overall residence time distribution in the proportion of its throughput. The proposed hydrodynamic model has been used to correlate our experimental data and that reported in the literature. The model satisfactorily describes both these data and provides a rational framework to predict the gas-phase behavior in bubble-column reactors.

Literature Review

While the liquid-phase axial backmixing in bubble columns has been extensively studied by many investigators (Baird and Rice, 1975; Deckwer et al., 1974; Joshi, 1980) over the past two decades and numerous empirical correlations and hydrodynamic models exist in the literature to predict the liquid-phase backmixing, very little has been studied about the gas-phase backmixing. A lack of data is due to the difficulty in measuring the gas-phase backmixing. A study of bubble-column performance requires an extensive and expensive experimental setup. Collection and analysis of experimental data also pose some special problems, particularly in the large end effects in the tracer detection system.

It is well established that the nonideal flow behavior of the phases in the reactor is responsible for a significant lowering of the reactor efficiency and should be accounted for to avoid improper reactor design and scale-up. The current trend is to describe the nonideal flow behavior with the help of an axial-dispersion model (ADM), which allows for the effect of longitudinal mixing on the reactor performance. The use of such a model for design purposes is not quite popular due to lack of reliable data on the gas-phase dispersion and the mass-transfer coefficient appearing in the model. Gas-phase backmixing data obtained by different researchers show considerable scatter as well as a difference in the experimental and predicted values. This scatter can be attributed to the different measurement and analysis techniques used. A primary reason for the difference in the experimental and predicted values is the underlying assumption of negligible mass transfer between the gas and liquid phases. In most of the cases, a simple one-dimensional axial-dispersion model was used without the inclusion of the mass-transfer term. Although all investigators (Towell and Ackermann, 1972; Joseph and Shah, 1986; Field and Davidson, 1980) observed tailing in their RTD curves, the analysis was done either by ignoring the tailing or by arbitrarily truncating the tailing at a certain point. The method of moments used by some of the investigators (Vanderlaan, 1957; Men'shchikov and Aerov, 1967; Towell and Ackermann, 1972) was criticized for its uncertainty in evaluating the tailing phenomenon (Radeke, 1981). Also, some unaccounted differences in the hydrodynamic, physico-chemical and mass-transfer conditions existing within the reactors of individual investigators might have introduced this scatter. A correct analytical model that includes mass-transfer effects, along with an accurate experimental technique, would alleviate the problem of inconsistent data on gas-phase backmixing.

The existing experimental work on gas-phase backmixing is summarized in Table 1. Most of the data lie in the homogeneous regime (in which the bubble sizes are relatively homogeneous). Data on the commercially important churn-turbulent regime are scarce. Based on rather limited experimental data, many empirical correlations have been proposed to predict the gas-phase dispersion coefficient in bubble column reactors. Joshi (1982) has reviewed the published literature on the gas-phase dispersion and shown that the existing correlations fit only a limited experimental data in each case. Shah et al. (1982) have recommended the correlations proposed by Joshi (1982) and Mangartz and Pilhofer (1981) to predict the gas-phase backmixing. Heijnen and Van't Riet (1984) have also reached a similar conclusion in their study on the gas-phase dispersion. Very little experimental data are available in literature regarding the effects of the physical and chemical properties of the gas and liquid phases on gas-phase backmixing. Towell and Ackermann (1972) have qualitatively discussed the effects of the physical and chemical properties of the gas and liquid phases on gas-phase backmixing. According to them, changing gas properties should have little effect since the buoyancy force is determined mainly by the liquid density; however, changing the liquid-phase properties would affect the mixing coefficients. Mangartz and Pilhofer (1981) observed a different dependence of the gas-phase dispersion on the superficial gas velocity in the homogeneous and churn-turbulent regimes for the air-water system; however, the dependence was uniform for other systems studied. Mikio and Tsutao (1988) estimated the gas-phase dispersion coefficients of large and small bubbles separately, and found the large bubbles to be more dispersed than the small bubbles in all the systems studied.

The effect of column internals on gas-phase dispersion has been studied by some researchers (Wachi and Nojima, 1990; Carleton et al., 1967; Kubo et al., 1970). Wachi and Nojima (1990) did not observe any effect at superficial gas velocities lower than 0.1 m/s. Studies by Kulkarni and Shah (1984) carried out in a downflow bubble column showed a weak dependence of gas-phase dispersion on superficial gas velocity and higher values of gas-phase dispersion coefficients than those observed in upflow systems. Literature on backmixing in gas-liquid reactors has been reviewed extensively by Shah et al. (1978).

According to Deckwer and Schumpe (1987), the current reactor modeling should be regarded as outmoded in view of the current knowledge of the fluid mechanics of the liquid phase and conditions existing in the gas phase. Greater progress can be expected in the field of design of bubble columns from the development of new theoretically based hydrodynamic models.

It was experimentally observed that at superficial gas velocities greater than the gas transition velocity, the gas holdup structure consists of two different bubble classes: the fast mov-

Table 1. Available Literature Data for Air-Water System in Bubble Columns

Reference	Column Diameter (m)	Dispersion Height (m)	Gas Velocity (m/s)	Liquid Velocity (m/s)
Carleton et al. (1967)	0.153	1.3	0.03 – 0.05	–
Diboun and Schugerl (1967)	0.135	0.42 – 0.52	0.0 – 0.06	0.0012 – 0.014
Field and Davidson (1980)	3.2	18.9	0.52	0.3 – 0.35
Joseph et al. (1985)	0.305	2.1	0.03 – 0.07	–
Kago et al. (1989)	0.12, 0.19	4.5	0.015 – 0.15	0.002 – 0.026
Kolbel et al. (1962)	0.092	0.7	0.04 – 0.07	–
Mangartz and Pilhofer (1981)	0.1, 0.14	0.7, 1.7	0.015 – 0.06	0.0 – 0.06
		0.6, 0.9	0.1	0.0 – 0.06
Men'shchikov and Aerov (1967)	0.3	5.0	0.0076 – 0.0096	–
Mikio and Tsutao (1988)	0.159, 0.29	2.0	0.02 – 0.12	–
Seher and Schumacher (1979)	0.45, 1.0	4.0	0.022	0.011
Towell and Ackermann (1972)	0.406, 1.067	2.84	0.016 – 0.13	0.0135
		5.1	0.008 – 0.034	0.0072
Wachi and Nojima (1990)	0.2, 0.5	4.5	0.029 – 0.456	–

Reference	Gas Tracer	Forcing Function	Gas Detector	Gas Sparger
Carleton et al. (1967)	Hydrogen	Pulse	Thermal conductivity cell	Sieve plate
Diboun and Schugerl (1967)	Helium	Pulse	Thermal conductivity cell	Sintered plate
Field and Davidson (1980)	Argon-41	Pulse	Scintillation counter	—
Joseph et al. (1985)	Nitrogen	Step	Polarographic sensor	Perforated plate
Kago et al. (1989)	Helium	Pulse	Thermal conductivity cell	Perforated plate
Kolbel et al. (1962)	—	—	—	—
Mangartz and Pilhofer (1981)	CH_4, CO, CO_2	Sinusoidal	Infrared gas detector	Sieve plate
Men'shchikov and Aerov (1967)	Hydrogen	Pulse	Thermal conductivity cell	Single tube
Mikio and Tsutao (1988)	Helium	Pulse	Thermal conductivity cell	Perforated plate
Seher and Schumacher (1979)	Argon-41	Pulse	Scintillation counter	Sieve plate
Towell and Ackermann (1972)	Freon-12	Pulse and step	Ionization cell	Single tube, eight point spider
Wachi and Nojima (1990)	Freon-12	Pulse	FID gas chromatograph	Perforated plate

ing large bubbles and small bubbles that are recirculating along with the liquid phase. Such a division of the gas into two bubble classes forms the starting point of the two-bubble-class model, introduced by Joseph and Shah (1984). They proposed that the two bubble classes behave differently as they move up in the column. They assumed that large bubbles travel in a plug-flow manner due to their high rise velocities, while the small bubbles tend toward complete backmixing due to the liquid recirculation. The mean residence of large bubbles is much smaller than that of small bubbles.

Many investigators (Sriram and Mann, 1977; Vermeer and Krishna, 1981; Schumpe and Deckwer, 1982; Godbole et al., 1982, 1984; Kelkar et al., 1983; Joseph and Shah, 1984; Schumpe and Grund, 1986; Molerus and Kurtin, 1986; Mikio and Tsutao, 1988; Patel et al., 1989) have also observed two distinct bubble classes in the churn-turbulent regime of operation in bubble columns. Vermeer and Krishna (1981) studied the hydrodynamics and mass transfer in the churn-turbulent regime in an organic liquid using the two-bubble-class model and concluded that the gas transport in this regime occurred exclusively due to large bubbles. Godbole et al. (1984a) have also studied the hydrodynamics and mass transfer in an organic liquid using the two-bubble-class model. Patel et al. (1989) have estimated the gas holdup structure, bubble rise velocities, bubble sizes and the gas-liquid interfacial area in the air-water system in bubble columns using the two-bubble-class model. Joseph and Shah (1984) applied the two-bubble-class model to model a simple, rapid, first-order reaction carried out in a bubble-column reactor.

All of the above researchers have used the dynamic gas disengagement (DGD) technique, which was first proposed by Sriram and Mann (1977), to measure the individual bubble-class holdups. This technique requires sophisticated equipment to monitor the dispersion height as a function of time after the gas supply has been stopped. Schumpe and Grund (1986) have discussed the problems associated with the DGD technique and have suggested measures to alleviate these problems. A simpler technique, which involves measuring the differential pressure between two points along the column length after a sudden shutdown in gas supply, has been used in this work. This method was first proposed by Molerus and Kurtin (1986).

Molerus and Kurtin (1986) have used the two-bubble-class model to generate a state diagram for the bubble column for the churn-turbulent regime of operation. They also used the two-bubble-class model to predict the bubble diameters, gas-liquid interfacial areas, and the liquid circulation velocities in the churn-turbulent regime of operation in bubble columns. Mikio and Tsutao (1988) have used the two-bubble-class model

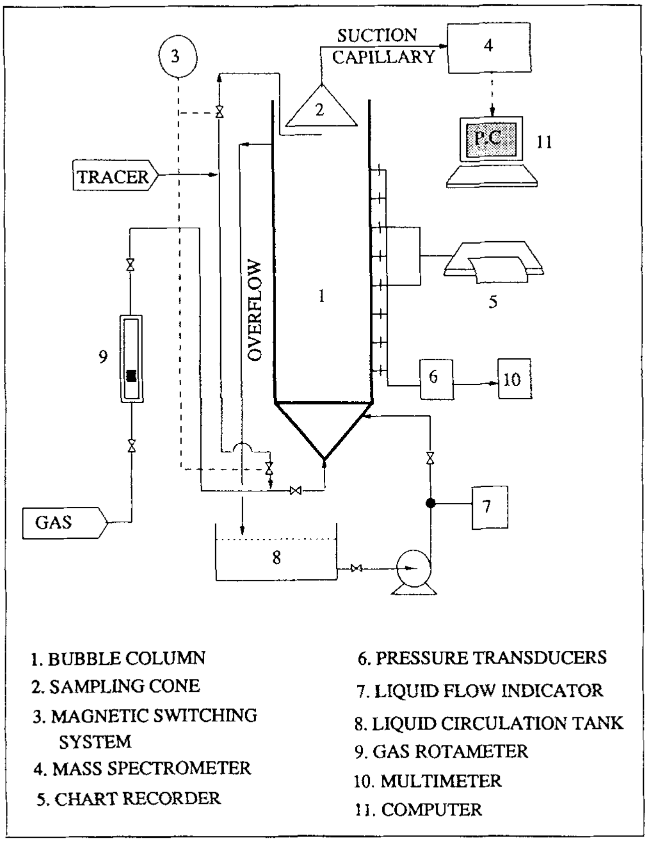

Figure 1. Experimental setup.

to describe the gas-phase dispersion in bubble columns. They used an optimization procedure to calculate the dispersion coefficients of the individual bubble classes as well as the fractional throughput of gas due to large bubbles. Based on the values obtained by the optimization procedure, Mikio and Tsutao (1988) concluded that 80% of the gas throughput was due to large bubbles and that large bubbles were more backmixed than small bubbles, an observation contrary to experimental observations (Vermeer and Krishna, 1981; Molerus and Kurtin, 1986).

Experimental Setup

Measurements were performed in two cylindrical, open-ended columns of 0.15 m and 0.25 m ID. These values were chosen because they were assumed to be large enough for the liquid phase to be completely backmixed. This considerably simplifies the analysis of data. The height of the test section was approximately 2.7 m and that of the whole column was 3.0 m. Both columns were constructed of transparent plexiglass to handle a variety of systems and to enable visual observation of the gas-in-liquid dispersion. Figure 1 shows the bubble column and measurement devices used.

All measurements were carried out with cocurrent upflow of both phases. The gas phase, air, was introduced at the bottom of the column through a perforated distributor plate after being metered with rotameters. A wire-mesh packing was provided below the distributor plate to avoid any possible maldistribution of gas at its entry point. The superficial gas velocity ranged from 0.01 to 0.16 m/s. The pressure in the gas inlet line was measured using pressure gauges. The liquid phase, tap water, was pumped from a storage vessel through the column and then recycled. The liquid flow rate was measured using a liquid flow rate indicator. The superficial liquid velocity varied from 0.005 to 0.03 m/s. Both columns were equipped with eight equally spaced connections for pressure transducers, each placed at a regular interval of 0.3 m along the column length.

Experimental data

For the measurement of the gas-phase backmixing, a pulse input of tracer was introduced at the bottom of the column using a fast switching magnetic valve. Switching times of the valve in the range of 1-5 ms proved sufficient. Preliminary experiments confirmed that the gas-phase tracer introduced at the bottom of the column appeared as a pulse input at the distributor with only a pure time delay. This delay was subtracted from all residence time distribution (RTD) data before further analysis. All RTD measurements of the gas phase were made using helium as the tracer in air. The gas disengaging from the surface of the gas-in-liquid dispersion was collected in an open-ended funnel kept as close as possible to the surface of the dispersion. This ensured that a representative sample of the gas was analyzed. In large columns (diameter greater than 1.0 m), it is impractical to have a cone of a correspondingly large size. A placement of the cone in off-center positions can ensure representative sampling.

A sensitive quadrupole mass spectrometer was used to measure the tracer concentration of the gas phase exiting the funnel. Sampling was done by a 50-μm-dia. capillary inlet probe. Preliminary experiments showed that the tracer collection/detection system, that is, the funnel and the capillary, had a RTD of their own, which was not a pure time delay. It was, therefore, necessary to correct the overall RTD data for the effect of the tracer collection detection system. Arrangements were, therefore, made to introduce helium just at the surface of the dispersion to measure the RTD of the tracer collection/detection system independently. For every run, the experimental data included the overall system RTD and the RTD of the tracer collection/detection system. Both of these raw RTD data measured by the mass spectrometer were transferred to and stored on a computer for further analysis.

The overall gas holdup was measured from the steady-state pressure profile obtained by using eight pressure transducers along the column length. The holdup of small gas bubbles was calculated from the steady-state pressure differential after a sudden shutdown in the gas supply to the column. The differential pressure measurement was made over a length of 0.6 m in the middle section of the column. A strip chart recorder equipped with a variable speed control unit was used to record the change in pressure drop with time after the gas supply was stopped. Figure 2 shows a typical differential pressure change with time after the sudden shutdown in gas supply. Pressure fluctuations observed initially correspond to the passage of large bubbles. Thereafter, a nearly constant value of the pressure differential is recorded which corresponds to the passage of only small bubbles. After the passage of the last small bubble at the lower transducer position, the pressure differential starts rising till it reaches a steady value corresponding to the static head of 0.6 m of water.

Data Analysis

It was concluded by Joseph and Shah (1986) that the assumption of negligible interphase transfer is valid only for tracer gases having high values of Henry's constant ($m > 1{,}000$). Even helium ($m = 106$), which is used as a gas tracer in this investigation, would not qualify as an insoluble tracer. Therefore, neglecting gas-liquid mass transfer can cause significant errors in the analysis of data. The actual residence time of the gas-phase tracer in the bubble column is greater than that based on the superficial gas velocity alone, because the gas phase is backmixed and some of the gas-phase tracer disappears into the liquid-phase because of tracer solubility. Neglecting tracer solubility attributes the entire delay in the appearance of the tracer to gas-phase backmixing and leads to a higher value than actual.

Gas-phase backmixing data obtained during the course of this work have been analyzed using a simple, one-dimensional, two-parameter axial-dispersion model (ADM) that takes into account the solubility of the gas-phase tracer into the liquid phase. The two parameters are the axial gas-phase dispersion coefficient that is a measure of the gas-phase backmixing and the volumetric mass-transfer coefficient that accounts for tracer gas solubility. The model describes the backmixing by a simple, one-dimensional Ficks-law type of diffusion equation characterized by a dimensionless form of the gas phase dispersion coefficient; expressed as the Peclet number (*Pe*). The value of *Pe* denotes the degree of backmixing, that is, complete backmixing as in an ideal CSTR if $Pe = 0$ and plug flow behavior as in an ideal PFR if $Pe = \infty$.

Mass balances of the reactant phases serve as the starting point for the model.

Mathematical formulation

A mass balance around a differential segment of the column disregarding radial variation and for the cocurrent mode of operation in the presence of mass transfer yields:

For the gas phase:

$$\epsilon_G D_G \frac{\partial^2 C_G}{\partial x^2} - U_G \frac{\partial C_G}{\partial x} - R = \epsilon_G \frac{\partial C_G}{\partial t} \tag{1}$$

For the liquid phase:

$$\epsilon_L D_L \frac{\partial^2 C_L}{\partial x^2} - U_L \frac{\partial C_L}{\partial x} + R = \epsilon_L \frac{\partial C_L}{\partial t} \tag{2}$$

The term R represents a mass flow and can be expressed based on whether the reaction is mass-transfer-controlled or kinetically-controlled. Data have been obtained only on the air-water system in this work. This is a case of physical absorption without chemical reaction, where

$$R = K_L a \{C_L^* - C_L\} \tag{3}$$

where C_L^* is the equilibrium interface concentration of the tracer and is related to the gas-phase concentration by Henry's law:

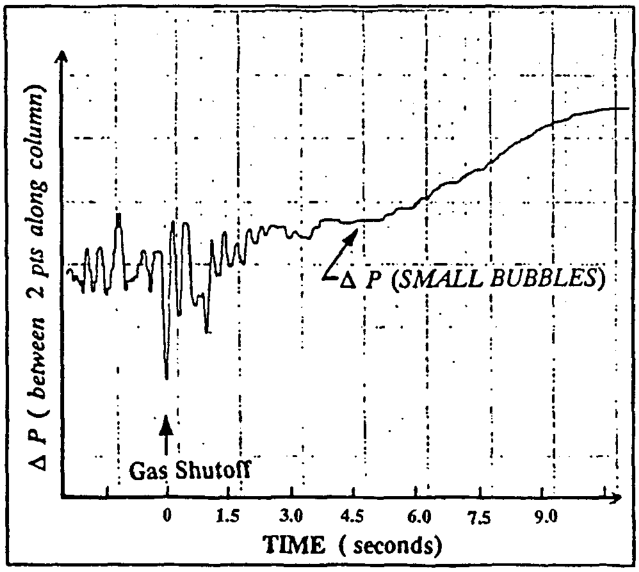

Figure 2. Typical differential pressure profile obtained after sudden shutdown in gas supply.

$$m C_L^* = C_G \tag{4}$$

where m is the Henry's constant. Substituting Eq. 3 in Eqs. 1 and 2 and appropriately defining dimensionless quantities, Eqs. 1 and 2 can be written, respectively, as:

$$\frac{1}{Pe_G}\frac{\partial^2 y}{\partial z^2} - \frac{\partial y}{\partial z} - \frac{St}{m}\{y - mc\} = \frac{\partial y}{\partial \theta} \tag{5}$$

$$\frac{U_r \cdot \epsilon_r}{Pe_L}\frac{\partial^2 c}{\partial z^2} - U_r \cdot \epsilon_r \frac{\partial c}{\partial z} + \frac{St \cdot \epsilon_r}{m}\{y - mc\} = \frac{\partial c}{\partial \theta} \tag{6}$$

with the initial condition at:

$$\theta = 0, \quad 0 < z < 1, \quad y = 0, \quad c = 0 \tag{7}$$

and boundary conditions at $z = 0$ and $\theta > 0$ for the gas phase:

$$y - \frac{1}{Pe_G}\frac{\partial y}{\partial z} = \begin{Bmatrix} \delta(\theta) & \text{(for a pulse input)} \\ 1 & \text{(for a step input)} \end{Bmatrix} \tag{8a}$$

and for the liquid phase:

$$c - \frac{1}{Pe_L}\frac{\partial c}{\partial z} = 0 \tag{8b}$$

and at

$$z = 1, \quad \theta > 0, \quad \frac{\partial y}{\partial z} = \frac{\partial c}{\partial z} = 0 \tag{8c}$$

In the above equations the dimensionless quantities defined are:

$$y=\frac{UC_G}{UC_f}\quad c=\frac{UC_H}{UC_f}\quad z=\frac{x}{H}\quad \theta=\frac{U_Gt}{H\epsilon_G}$$

$$Pe_G=\frac{HU_G}{D_G\epsilon_G}\quad St=\frac{HK_La}{U_G}\quad U_r=\frac{U_L}{U_G}\quad \epsilon_r=\frac{\epsilon_G}{\epsilon_L}$$

where y is the dimensionless gas-phase tracer concentration and c is the dimensionless tracer concentration in the liquid phase.

The analysis of data can be considerably simplified by assuming the liquid phase to be completely backmixed (Nakanoh and Yoshida, 1980; Towell and Ackermann, 1972). Joseph and Shah (1986) have also shown this to be a justified assumption for bubble columns with diameter greater than 0.14 m. Based on this assumption, Eq. 6 simplifies to:

$$-U_r\epsilon_r c+\frac{St.\epsilon_r}{m}\int_0^1 (y-mc)dz=\frac{dc}{d\theta} \tag{9}$$

with initial and boundary conditions given by Eqs. 7, 8a, 8b and 8c.

The difficulty of solving Eqs. 5 and 9 analytically in the time domain can be overcome by solving them simultaneously in the Laplace domain (Shetty, 1991). However due to the complexity of the solution, it is impossible to analytically invert the solution into the time domain. The equations were therefore numerically inverted using the Stehfest algorithm (Stehfest, 1970), which is simple to use and has been shown to match well with the analytical solution given by Brenner (1962).

Before fitting the raw experimental data into the reactor model, the measured overall RTD must be corrected for the effects introduced by the tracer collection/detection system. This was done by deconvoluting the response obtained by introducing a tracer at the dispersion surface from the response of the overall system. If $E_0(t)$, $E(t)$, and $E_m(t)$ are the RTDs of the overall system, the gas-liquid dispersion, that is, the bubble column alone, and the tracer collection/detection system, respectively, then the desired relationship can be expressed using the convolution integral (Levenspiel, 1972).

$$E_o(t)=\int_0^t E(t)\cdot E_m(t-t_0)dt_0 \tag{10}$$

Applying the Fourier transform to Eq. 10,

$$e_o(\omega)=e(\omega)\cdot e_m(\omega) \tag{11}$$

where $e_o(\omega)$ is the image function of $E_o(t)$ in the Fourier space, therefore

$$e(\omega)=\frac{e_o(\omega)}{e_m(\omega)} \tag{12}$$

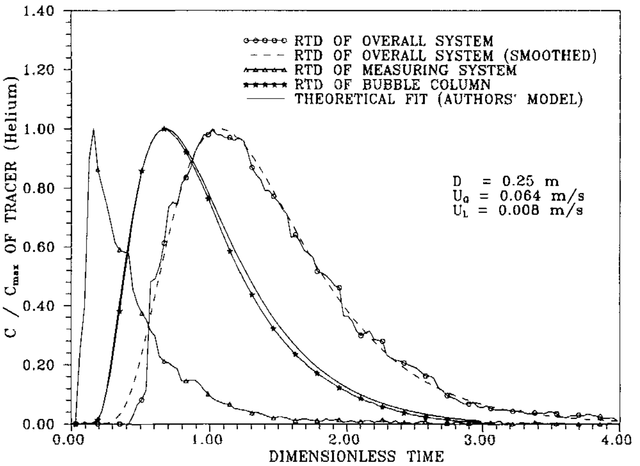

Figure 3. Typical raw experimental RTD curves for the overall system.

A computer program was used to compute the discrete fast Fourier transform (FFT) of both the overall system RTD and the tracer collection/detection system RTD and then deconvolute the latter from the former by a complex division in Fourier space. The corrected RTD of the bubble column was obtained by an inverse FFT of the quotient $e(\omega)$ back to the time domain (Lubbert, 1990). It was found that this deconvolution step was very sensitive to noise in the raw experimental data. Therefore, the data had to be smoothed. This was done by fitting the overall system response to a simple, one-dimensional axial-dispersion model (Levenspiel, 1972). In addition to the two model parameters, the mean residence time, τ, and the Bodenstein number, Bo, it was necessary to take into account the baseline level, bl, and the amplitude, amp, of the experimental RTD curve. A nonlinear numerical optimization routine based on the method of Nelder and Mead (1965) was used to fit the raw experimental data to a smooth profile given by:

$$E(\theta)=bl+\text{amp}^*\left(\sqrt{\frac{\tau.Bo}{4^*\pi^*\theta}}\exp\left(\frac{-Bo(t-\tau)^2}{4^*\tau^*\theta}\right)\right) \tag{13}$$

There was no need to smooth the tracer collection/detection system response, since this experimentally observed response was quite smooth to be accepted by the deconvolution procedure.

A Levenberg-Marquardt-type nonlinear parameter optimization scheme (Press et al., 1986) was used to obtain the experimental Peclet number and Stanton number by fitting the corrected column response to the reactor model (Eqs. 5 and 9). Initial guesses for the two parameters need to be given. The numerical procedure then optimizes them till the sum of the squares of the difference (Chisq) between the experimental and generated profiles (from the reactor model) is minimized. Chisq values obtained were typically in the range of 0.01-0.1 for a RTD involving 100 concentration vs. time data points. The reactor model was found to be sensitive to the Peclet number, but for the tracer used, helium, the model was found to be insensitive to the Stanton number. This method of analysis results in obtaining not only the gas-phase dispersion coefficient but also the volumetric mass-transfer coefficient. Figure 3 shows typical raw experimental RTD curves for the overall system with its smooth profile obtained using Eq. 13, the tracer collection/detection system, the deconvolution result obtained after correcting for the tracer collection/detection system and the fit obtained using our reactor model.

The measurement of gas holdup was simple and could be easily obtained from the steady-state pressure profile along the

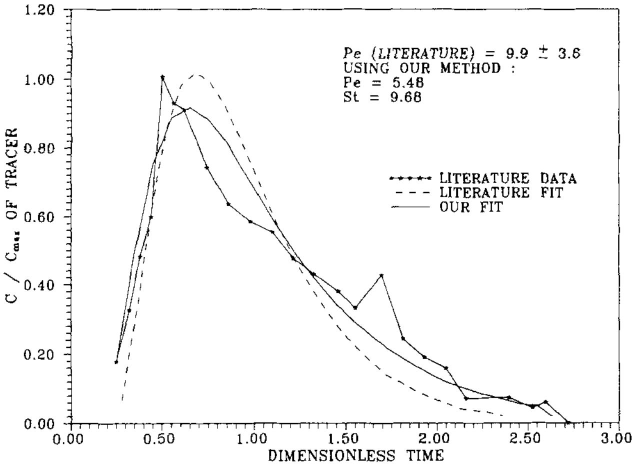

Figure 4. Match between the model's simulated data and Davidson's experimental data.

column length. A simple, steady-state momentum balance in terms of the hydrostatic pressure yields:

$$-\frac{dp}{dx}=(\rho_L\epsilon_L+\rho_G\epsilon_G)\,\frac{g}{g_c} \tag{14}$$

Knowing $\epsilon_L = 1 - \epsilon_G$, gas holdup can be easily calculated.

Equation 14 can also be used to calculate the small bubble holdup knowing the differential pressure corresponding to the passage of small bubbles over 0.6 m of column length. Defining $\epsilon_L = 1-\epsilon_{G_1}$ for the small bubbles-liquid dispersion, the small bubble holdup can also be calculated.

Analysis of literature data

The applicability of the proposed reactor model and the method of analysis were verified by re-analyzing existing literature data on gas-phase dispersion using the method proposed in this work. Data reported by Field and Davidson (1980) and by Towell and Ackermann (1972) were used for this analysis. Figure 4 shows the match between the simulated data using our model and Field and Davidson's experimental data and their fit along with the estimated values of Peclet and Stanton numbers (estimated values were obtained using our model). The ability of our model to fit the peak better indicates that it matches the mean residence time of the tracer quite accurately. Matching of the tail of the RTD curve indicates that any tracer absorption effects are also accounted for. This conforms with the literature evidence that any tracer absorption effects show up mainly in the tail of the RTD curve. Significantly different values of the estimated Peclet number from those reported by Field and Davidson show that their assumption of negligible interphase mass transfer may not be accurate. Experimental data given by Towell and Ackermann (1972) were also analyzed using our model (see Figure 5).

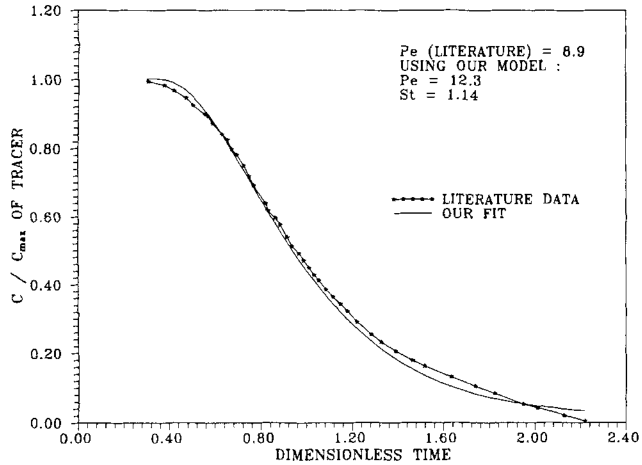

Figure 5. Experimental data of Towell and Ackermann (1972) analyzed using our model.

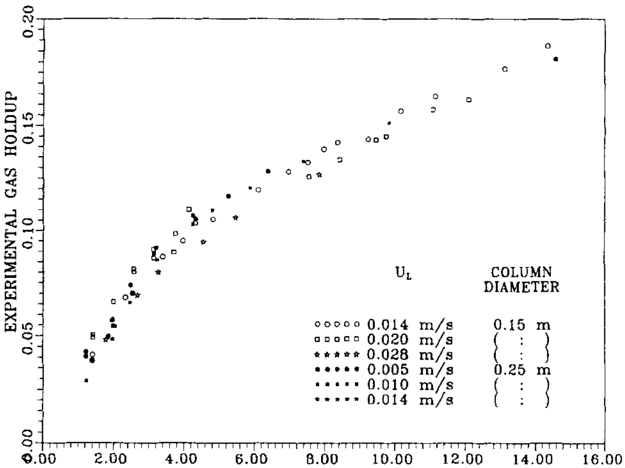

Figure 6. Gas holdup independent of superficial liquid velocity and column diameter, but dependent on superficial gas velocity.

The ability of the proposed model to match the mean residence time and the tailing of the RTD curve, therefore, eliminates the need to truncate the RTD curves arbitrarily.

Results and Discussion

While the primary aim of this investigation was to study and measure the gas-phase backmixing in the bubble column reactors, two other parameters, the gas holdup and the volumetric mass-transfer coefficient, were also studied. The operating variables included the column diameter and the superficial gas-and liquid-phase velocities.

Gas holdup

Figure 6 shows that the gas holdup is not dependent on the superficial liquid velocity and the column diameter in the range studied, but varies with the superficial gas velocity. The relative increase in gas holdup with the superficial gas velocity is lower in churn-turbulent regime than in the homogeneous regime, due to higher bubble coalescence and faster bubble rise velocities. Shah et al. (1982) have reviewed the effect of various operating parameters on the gas holdup along with a large number of correlations to predict it. The experimental data agrees well with the correlations proposed by Akita and Yosh-

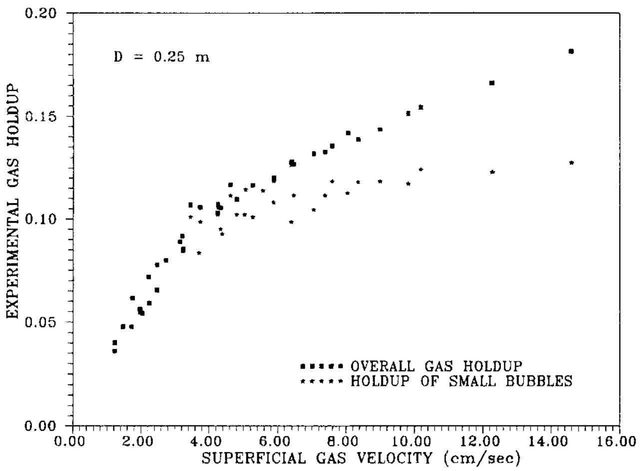

Figure 7. Fractional gas holdup of individual bubble classes as a function of superficial gas velocity.

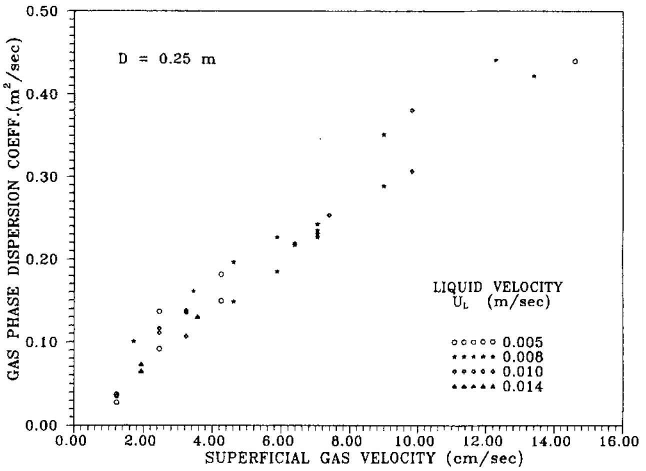

Figure 9. Effect of superficial liquid velocity on gas-phase dispersion.

ida (1973) and Hikita et al. (1980). Since the gas holdup is independent of the column diameter above 0.15 m, the results obtained in small laboratory-scale columns can be applied to large-scale industrial columns for the same superficial gas velocity.

Figure 7 shows the fractional holdups of the individual bubble classes as a function of the superficial gas velocity. At higher gas velocities, an increase in bubble coalescence and major gas transport via large bubbles explains the leveling of the small bubble holdup.

Gas-Phase backmixing

It was observed that the gas-phase backmixing depends on the superficial gas velocity and the column diameter; the effect of column diameter being more pronounced after the transition into the churn-turbulent regime (Figure 8). The superficial liquid velocity, however, had no effect over the range studied (Figure 9). The dependence can be explained by examining the possible causes of gas-phase dispersion. At low gas velocities, the swarm of bubbles rise uniformly without being hindered either by the column wall or by the presence of other bubbles. At higher gas velocities, however, bubble clusters are formed, flow becomes heterogeneous, and intense liquid recirculation is observed. Large bubbles or bubble agglomerates, the sizes of which are limited by the column wall, ascend in the core region. In the outer annulus (near the wall), downward motion is observed and bubbles with terminal rise velocity less than the liquid recirculation velocity are entrained in the downward moving liquid. The energy for the liquid recirculation is provided by the introduction of the gas phase. The superficial gas velocity is therefore the controlling velocity.

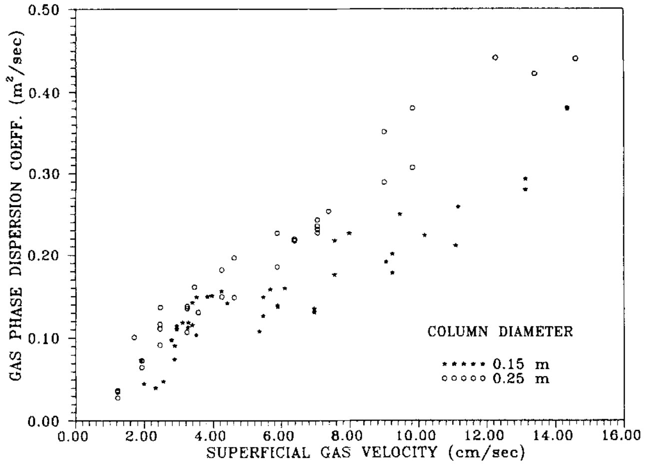

Figure 8. Effect of column diameter and superficial gas velocity on gas-phase dispersion.

Gas-phase backmixing also depends on the column diameter. In the homogeneous regime there is no significant movement of the gas phase in the radial direction, and the effect of column diameter is not significant. At high gas velocities, the gas phase can disperse in the axial direction (along the column length) as well as along the radial direction, this length being limited by the column diameter. The colum diameter being the smaller of the two is therefore the primary scale length which determines the extent of gas-phase dispersion by controlling the heterogeneity created in the column due to liquid recirculation. In industrial applications, the superficial liquid velocity is usually much lower than the superficial gas velocity. Also, the variations in liquid velocities do not significantly affect the liquid recirculation and hence the gas-phase backmixing (Joshi et al., 1986). The bubble rise velocity relative to the column wall is more important than the slip velocity of the gas with respect to the liquid phase.

Experimental gas-phase dispersion coefficients have been compared with the literature correlations (Figure 10). Considerable disparity exists among the values predicted by the existing empirical correlations. A more fundamental approach toward predicting gas-phase backmixing is therefore needed. A new hydrodynamic model to predict gas-phase backmixing has been proposed in this article.

Volumetric mass-transfer coefficient

The reactor model was found to be insensitive to the Stanton number. The Stanton number and hence the volumetric mass-

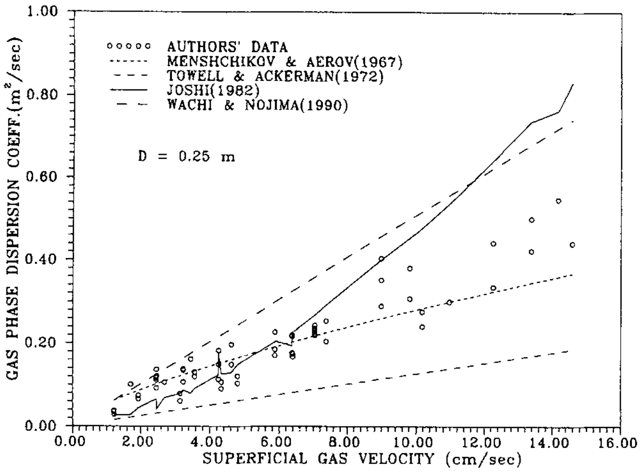

Figure 10. Experimental and literature gas-phase dispersion coefficients.

transfer coefficient (K_La) values obtained during this work are therefore not professed to be accurate. They are, however, representative of the K_La values typically observed in the bubble columns. The experimental results agree qualitatively with the data reported in literature. It appears that the K_La is independent of the superficial liquid velocity and the column diameter, but is a function of the superficial gas velocity (Figure 11). Deckwer et al. (1974) have proposed an empirical correlation of the type, $K_La = b^* U_G^n$ with the values of $b = 1.174$ and $n = 0.82$ for the air-water system. For data obtained during this investigation, $b = 3.361$ and $n = 1.118$.

The insensitivity of the reactor model toward the Stanton number can be explained on the basis of the system studied. The tracer used, helium, being very sparingly soluble in water, no significant mass-transfer effects appear in the tail of the RTD curve. We think that with the use of gas tracers having high solubilities, the reactor model would be able to estimate the Stanton number more accurately.

In addition to the superficial gas velocity, the volumetric mass-transfer coefficient is sensitive to the physico-chemical properties of the system, particularly those which promote or prevent coalescence. A generalized correlation for the prediction of K_La is, therefore, not possible. The results obtained on small-scale columns however, can be used for designing large-scale columns with operating parameters being kept same.

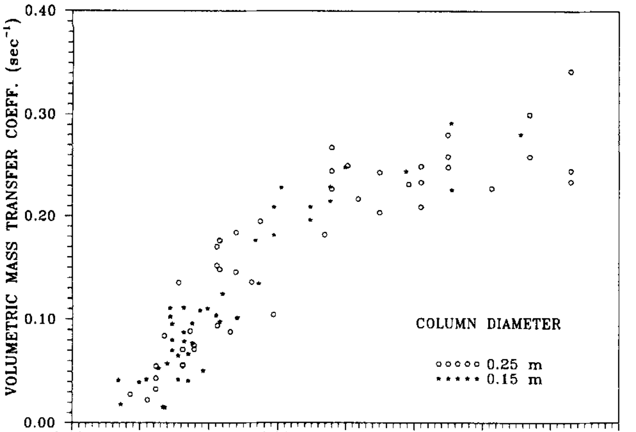

Figure 11. Volumetric mass-transfer coefficient as a function of superficial gas velocity.

Two-Bubble-Class Hydrodynamic Model to Predict Gas-Phase Backmixing

A two-bubble-class hydrodynamic model to predict gas-phase backmixing in bubble columns has been proposed in this section. The model needs only easily obtainable parameters to generate the RTD profile of the gas phase in the bubble column. Its primary advantage over a reactor model like the ADM is that it does not need any experimental RTD data to predict the gas-phase dispersion coefficient.

The following assumptions have been made in developing the hydrodynamic model; most of these being supported by previous investigations.

1) The large bubbles are assumed to travel in a plug-flow manner.

2) The small bubbles are assumed to be partially backmixed. Since they are recirculated along with the liquid-phase circulations, it is assumed that their backmixing coefficient equals those of the liquid phase.

3) The variation in gas flow rate due to a drop in pressure along the column length is assumed to be negligible.

4) There are no axial variations in the gas holdup.

5) The equilibrium liquid-phase concentration of the gas-phase tracer in both large and small bubble classes is given by Henry's law: $mC_L^* = C_G$, where m is the Henry's constant.

6) There is no interaction between the two-bubble classes.

7) The fraction of the total liquid holdup associated with each bubble phase is proportional to the gas-phase holdup of that particular bubble phase:

$$\frac{\epsilon_{G_1}}{\epsilon_{G_2}} = \frac{\epsilon_{L_1}}{\epsilon_{L_2}} \tag{15}$$

Figure 12 shows a schematic representation of the two-bubble classes in the column.

The overall residence time distribution, $E(t)$, of the gas phase in the bubble column can be written as:

$$E(t) = \alpha E_2(t) + (1-\alpha)E_1(t) \tag{16}$$

where $E_1(t)$ and $E_2(t)$ are the residence time distributions (RTD) of small bubble and large bubble phases, respectively, and

$$\alpha = \frac{U_{G_2}}{U_G} \tag{17}$$

where U_{G_2} is the superficial velocity of the large bubbles and U_G is the overall superficial gas velocity.

The RTDs of the individual bubble classes are obtained by solving the mass-balance equation for the gas-phase tracer in the gas phase and the liquid phase for each bubble class separately.

For the small bubbles, which are assumed to be partially backmixed, mass balances are given as follows.

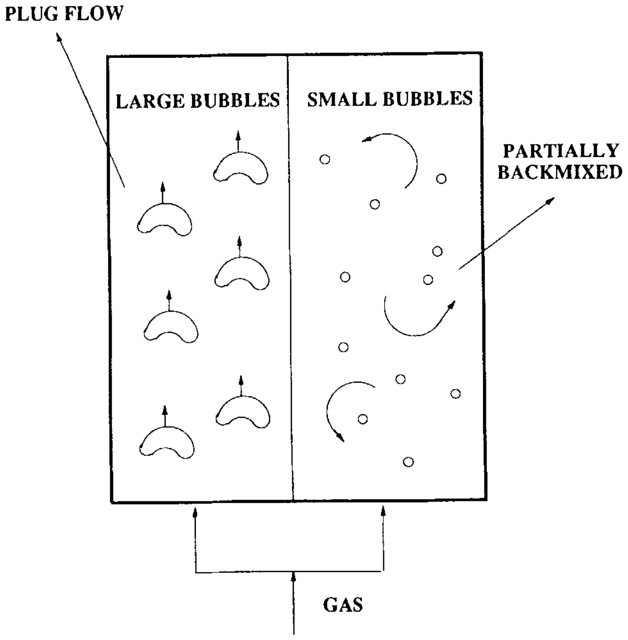

Figure 12. Two bubble classes in a bubble-column reactor.

For the gas phase in the form of small bubbles:

$$\epsilon_{G_1} D_{G_1} \frac{\partial^2 C_{G_1}}{\partial x^2} - U_{G_1} \frac{\partial C_{G_1}}{\partial x} - R_1 = \epsilon_{G_1} \frac{\partial C_{G_1}}{\partial t} \tag{18}$$

where

$$R_1 = (K_L a)_1 (C^*_{L_1} - C_{L_1})$$

For the liquid phase associated with small bubbles:

$$\epsilon_{L_1} D_{L_1} \frac{\partial^2 C_{L_1}}{\partial x^2} - U_L \frac{\partial C_{L_1}}{\partial x} + R_1 = \epsilon_{L_1} \frac{\partial C_{L_1}}{\partial t} \tag{19}$$

It should be noted that the small-bubble holdup used in Eq. 18, ϵ_{G_1}, is obtained after correcting the experimentally obtained small-bubble holdup, $\epsilon_{G_{1m}}$, for the presence of large bubbles. When the small-bubble holdup is experimentally measured, only small bubbles and the liquid phase exist in the column, therefore

$$\epsilon_{G_{1m}} = \frac{V_1}{V_1 + V_L} \tag{20}$$

where V_1 is the volume of the small bubble phase.
The actual small-bubble holdup in the operating column is defined by:

$$\epsilon_{G_1} = \frac{V_1}{V_G + V_L} \tag{21}$$

Using Eqs. 20 and 21

$$\epsilon_{G_1} = \frac{\epsilon_{G_{1m}}(1 - \epsilon_G)}{1 - \epsilon_{G_{1m}}} \tag{22}$$

$$\epsilon_{G_2} = \epsilon_G - \epsilon_{G_1} \tag{23}$$

The fraction of the liquid holdup associated with each bubble phase can be calculated according to assumption 7. Using

$$\epsilon_{G_1} + \epsilon_{G_2} + \epsilon_{L_1} + \epsilon_{L_2} = 1$$

and Eq. 15,

$$\epsilon_{L_1} = \frac{(1 - \epsilon_{G_1} - \epsilon_{G_2})}{\left(1 + \dfrac{\epsilon_{G_2}}{\epsilon_{G_1}}\right)} \tag{24}$$

$$\epsilon_{L_2} = \frac{(1 - \epsilon_{G_1} - \epsilon_{G_2})}{\left(1 + \dfrac{\epsilon_{G_1}}{\epsilon_{G_2}}\right)} \tag{25}$$

Large bubbles are assumed to be in plug flow, in which the mass-balance equations reduce to Eqs. 26 and 27.
For the gas phase in the form of large bubbles:

$$-U_{G_2} \frac{\partial C_{G_2}}{\partial x} - R_2 = \epsilon_{G_2} \frac{\partial C_{G_2}}{\partial t} \tag{26}$$

where

$$R_2 = (K_L a)_2 (C^*_{L_2} - C_{L_2})$$

For the liquid phase associated with large bubbles:

$$\epsilon_{L_2} D_{L_2} \frac{\partial^2 C_{L_2}}{\partial x^2} - U_L \frac{\partial C_{L_2}}{\partial x} + R_2 = \epsilon_{L_2} \frac{\partial C_{L_2}}{\partial t} \tag{27}$$

The mass balance for small and large bubbles are solved in the Laplace space using the procedure described earlier. Solving Eqs. 18 and 19 gives $E_1(t)$, the RTD of small-bubble phase, and solving Eqs. 26 and 27 gives $E_2(t)$, the RTD of large-bubble phase.

The model parameters include the gas-phase dispersion coefficient for small bubbles, individual bubble class holdups, individual volumetric mass-transfer coefficients, and α. Of all these parameters, only small and large bubble holdups were measured experimentally.

The dispersion coefficient of small bubbles is taken to equal the dispersion coefficient for the liquid phase (assumption 2). Abundant data exist in the literature for the prediction of the liquid-phase dispersion coefficient. The widely used correlation proposed by Deckwer et al. (1974) was used to calculate the dispersion coefficient of small bubbles in this work.

$$D_{G_1} = D_L = 0.678 D^{1.4} U_G^{0.3} \tag{28}$$

It is necessary to know the fractional holdups of small and large bubbles to use the two-bubble-class model. No reliable correlations exist as yet in the literature to predict the small-bubble holdup. Reliable values of the fractional holdups can be obtained only experimentally. The experimental measurements can be done on a small-scale column, since the gas holdup is not dependent on the column diameter. This result was also confirmed by the gas holdup data obtained during this study. The values of the liquid-side mass-transfer coefficients for small and large bubble classes, K_{L1} and K_{L2}, have been reported by Joseph and Shah (1984) as $K_{L1} = 0.0074$ cm/s and $K_{L2} = 0.031$ cm/s. The interfacial areas $\underline{a}_1$ and $\underline{a}_2$ were calculated by the following equations:

$$\underline{a}_1 = \frac{6\epsilon_{G_1}}{d_{b_1}} \qquad \underline{a}_2 = \frac{6\epsilon_{G_2}}{d_{b_2}}$$

where d_{b_1} and d_{b_2} are the diameters of small and large bubbles. The small-bubble diameter could be visually estimated to be 0.001 to 0.003 m. The small-bubble diameter can be assumed to remain constant with superficial gas velocity. The values of the diameter of large bubbles in the air-water system have been reported by Joseph and Shah (1984), as a function of the overall superficial gas velocity. As will be shown later, no significant errors are introduced by using the above estimated values since the model has been shown to be insensitive to the individual volumetric mass-transfer coefficients.

The evaluation of α needs the knowledge of the superficial gas velocities of small and large bubble phases. A simple mass balance across any cross-section of the column gives for a cocurrent flow:

$$\frac{U_{G_i}}{\epsilon_{G_i}} - \frac{U_L}{1-\epsilon_{G_i}} = U_{b_{r_i}} \tag{29}$$

where i indicates the individual bubble phases.

The large-bubble rise velocity, $U_{b_{r_2}}$, was calculated by using the differential pressure-time profile obtained using the dynamic disengagement technique employed in this investigation (Figure 2). Shortly after shutting off the gas flow to the column, the initial rise in the pressure drop till it reaches a steady value (which corresponds to the presence of only small bubbles) indicates that large bubbles are disengaging from the test section. The rise velocity of large bubbles is then calculated knowing the time required for the last large bubble to disengage and the distance it has traveled which was 1.9 m. The time required for the last large bubble to disengage was obtained knowing the chart speed and the span of the initial rise of the pressure differential.

Knowing the large-bubble rise velocity, $U_{b_{r_2}}$, and individual phase holdups, the superficial velocity of large bubbles can be calculated from Eq. 29:

$$U_{G_2} = \left(U_{b_{r_2}} + \frac{U_L}{1-\epsilon_{G_2}}\right) \cdot \epsilon_{G_2} \tag{30}$$

The superficial velocity of small bubbles can be calculated by:

$$U_{G_1} = U_G - U_{G_2} \tag{31}$$

The bubble rise velocity of small bubbles, $U_{b_{r_1}}$, can now be calculated from Eq. 29 and α can be calculated using Eq. 17. Typical values of breakthrough time observed experimentally agreed well with the values obtained based on the calculated bubble rise velocity. Bubble breakthrough time is the time required for the first bubble of gas, injected at the distributor, to appear at the surface of the gas-in-liquid dispersion.

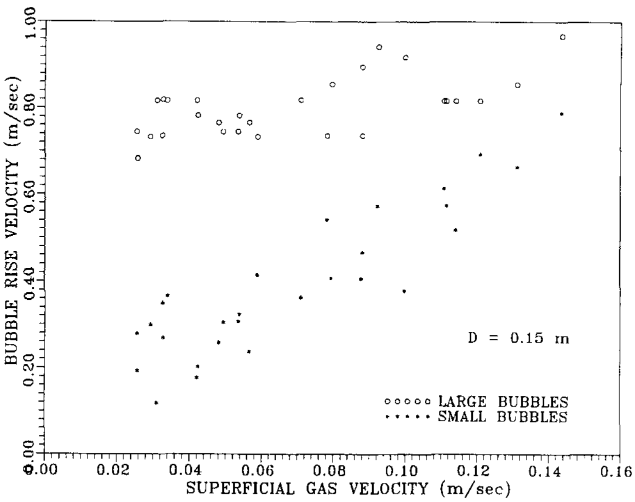

Figure 13. Bubble rise velocities as a function of overall superficial gas velocity.

Figure 13 shows large and small bubble rise velocities as a function of the overall superficial gas velocity. The nature of the residence time distribution profile predicted depends on the values of α. A value of $\alpha = 0$ implies that only small bubbles exist: the flow is in the homogeneous regime. A value of $\alpha = 1$ implies that all the gas throughput is in the form of large bubbles and the gas-phase flows in a plug-flow manner.

Effect of Model Parameters on the Predicted Residence Time Distribution Profile

It is necessary to measure the individual bubble class holdups accurately, since the value of α depends directly on them. A higher value of the large-bubble holdup implies a larger throughput of the gas in the form of large bubbles and will give a higher value of α than actual. A tenfold variation in the volumetric mass-transfer coefficients had no effect on the residence time distribution profile predicted using the two-bubble-class model. Although the dispersion coefficient of small bubbles should be taken to equal that of the liquid phase, no appreciable difference in the predicted residence time distribution profiles is observed by using different available literature correlations (Field and Davidson, 1980; Joshi and Sharma, 1979; Towell and Ackermann, 1972; Deckwer et al., 1974) to calculate the liquid-phase dispersion coefficient.

Validation of the Two-Bubble-Class Model

The validity of the proposed model has been verified by comparing the residence time distribution profiles predicted using the proposed model with residence time distribution data available in literature as well as our own experimental data.

The residence time distribution profile, predicted using the two-bubble-class model, has been compared with the data reported by Mikio and Tsutao (1988). The values of α and the fractional holdups of small and large bubbles are taken from the literature data. Figure 14 shows the residence time distribution of small bubbles only ($\alpha = 0$), because the superficial

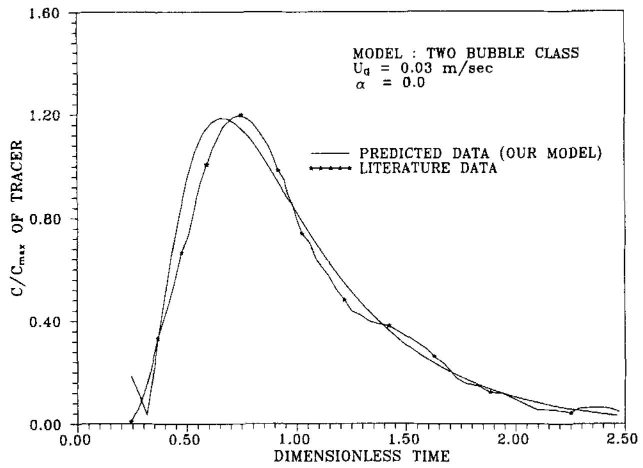

Figure 14. Residence time distribution of small bubbles.

gas velocity of 0.03 m/s was low enough to be in the homogeneous regime. Other comparisons of the published data are shown by Shetty (1991). The predicted residence time distribution profiles are seen to agree well with the literature data. The proposed model was also used to correlate our own experimental data. Figure 15 shows the comparison between the predicted and the experimental profile for a superficial gas velocity of 0.15 m/s. Similar matches are observed at other gas velocities (Shetty, 1991).

Optimized values of α were also calculated by fitting the experimental RTD to Eq. 16. Individual RTDs $E_1(t)$ and $E_2(t)$ were generated by solving Eqs. 18, 19, 26 and 27. The optimized values of α so obtained correspond to the best fit between the experimental RTD and the RTD generated using the proposed model. Figure 16 shows the predicted and best-fit values of α. The values match well with each other, indicating that the results from the proposed model will agree well with the experimental RTD for the gas phase.

Summary

The procedure for predicting the residence time distribution profile of the gas phase in bubble columns using the proposed two-bubble-class model is as follows. The model requires a knowledge of the total gas holdup, the individual bubble class holdups, and the individual volumetric mass-transfer coefficients.

1) Measure the overall gas holdup and fractional gas holdup of small and large bubbles. Experimental measurements can be done on a small-scale column using a simple procedure.

2) The large bubble rise velocity is calculated from the presure differential profile obtained after sudden shutdown in the gas supply.

3) The superficial gas velocity of large bubbles is calculated using Eq. 30.

4) The superficial gas velocity of small bubbles can then be calculated from Eq. 31.

5) Calculate α from Eq. 17.

6) The individual residence time distributions of small- and large-bubble classes can be generated by solving Eqs. 18, 19, 26 and 27. The dispersion coefficient of small bubbles is taken to equal the dispersion coefficient of the liquid phase. The values of individual volumetric mass-transfer coefficients have been given in the literature.

7) The overall residence time distribution profile for the gas phase can be generated using Eq. 16.

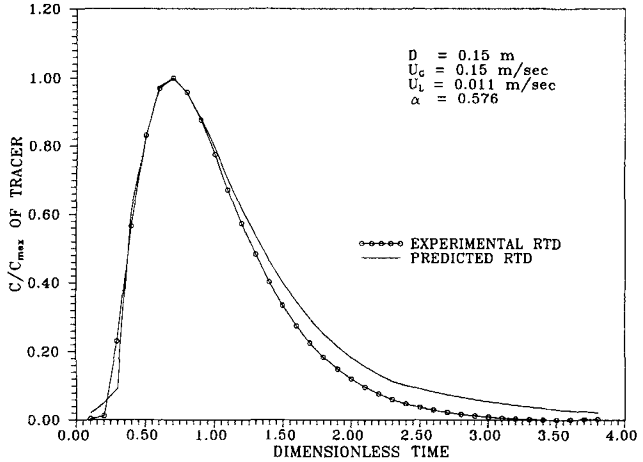

Figure 15. Predicted and experimental profile for a superficial gas velocity of 0.15 m/s.

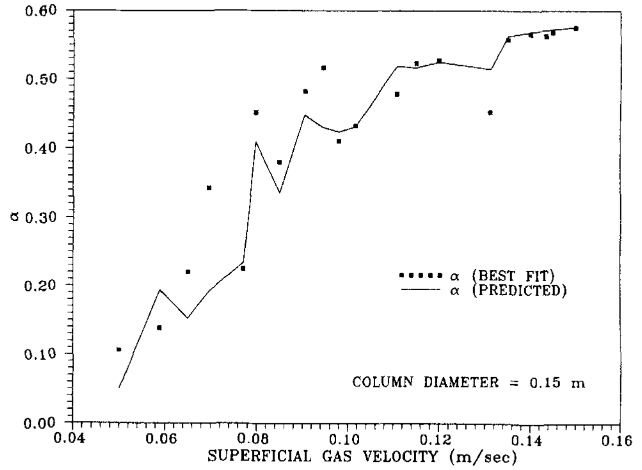

Figure 16. Optimized values of α.

Conclusions and Recommendations

According to our experimental data, neglecting the gas-phase tracer solubility, even for a sparingly soluble gas-like helium in water, gives higher than actual gas-phase dispersion values, thus leading to an overdesign in the bubble column reactor volume. In analyzing the experimental RTD data, it is imperative to correct for the effect of the tracer measurement system. The gas-phase backmixing, gas holdup, and volumetric mass-transfer coefficient depend strongly on the superficial gas velocity. Gas-phase backmixing was the only parameter affected by the column diameter, the influence being more significant at high gas velocities. The superficial liquid velocity was not high enough to affect any of the three parameters studied.

More experimental data on gas-phase backmixing is required at higher superficial gas velocities, particularly in the commercially important churn-turbulent regime. The effect of physico-chemical properties on gas-phase backmixing also need to be studied.

The two-bubble-class hydrodynamic model satisfactorily predicts the gas-phase backmixing in bubble columns. The number of parameters required by the model are small and can be easily evaluated under a wide range of operating conditions. The model also provides a more realistic description of the gas-phase backmixing and allows a more reliable scale-up of the reactor than the conventional single-bubble-class model. While no interaction between the two bubble classes has been assumed in this work, it is known that the bubble coalescence and breakage significantly affect the gas-phase dispersion. Future modeling using the two-bubble-class model should incorporate the effects of these bubble-bubble interactions. The validity of the two-bubble-class model for systems other than air-water, where two distinct bubble classes are observed, should be verified.

Experimental data along with a more fundamental approach to interpreting it will lead to solutions of the various scale-up problems encountered in bubble-column design today.

Acknowledgment

The financial support by the National Science Foundation for this study is gratefully acknowledged. The University of Tulsa provided the laboratory and computer facilities for this work.

Notation

a = gas-liquid interfacial area, m^2/m^3
amp = amplitude used in Eq. 13
bl = nondimensional base level of the experimental RTD curve
Bo = Bodenstein number used in Eq. 13
c = normalized liquid-phase tracer concentration
C = concentration of tracer, kmol/m^3
C_f = reference concentration of tracer, kmol/m^3.
d_b = bubble diameter, m
D = column diameter, m
D_G = gas-phase dispersion coefficient, m^2/s
D_L = liquid-phase dispersion coefficient, m^2/s
$E(t)$ = nondimensional residence time distribution curve
$e(\omega)$ = image function of $E(t)$ in the Fourier space
g = acceleration due to gravity, m/s^2
g_c = gravitational constant, kg·m/s^2/kgf
H = gas-in-liquid dispersion height, m
K_L = liquid-side true mass-transfer coefficient, m/s
K_La = liquid-side volumetric mass-transfer coefficient, s^{-1}
m = Henry's law constant, m^3(liq)/m^3(gas)
M = enhancement of mass transfer due to chemical reaction
P = hydrostatic pressure, kgf/m^2
Pe = Peclet number
R = rate of mass transfer, kmol/m^3/s
St = Stanton number
t = time, s
U = superficial phase velocity, m/s
U_{br} = bubble rise velocity, m/s
U_r = dimensionless velocity
V = volume, m^3
x = distance along the column length, m
y = dimensionless gas phase tracer concentration
z = dimensionless distance along column length

Greek letters

α = ratio of superficial gas velocity of large bubbles to overall superficial velocity
$\delta(\theta)$ = Dirac delta function
ϵ = phase holdup
ϵ_r = relative phase holdup
ρ = phase density, kg/m^3
τ = mean residence of tracer in the column, s
ω = variable in the Fourier space
θ = dimensionless time

Subscripts

G = gas phase
i = individual bubble phase
L = liquid phase
m = measurement system
max = maximum value
o = overall system
1 = small bubble phase
2 = large bubble phase

Literature Cited

Akita, K., and Y. Yoshida, "Gas Holdup and Volumetric Mass-Transfer Coefficient in Bubble Columns," *Ind. Eng. Chem. Proc. Des. Dev.*, **12**, 76 (1973).

Baird, M. H. I., and R. G. Rice, "Axial Dispersion in Large Unbaffled Columns," *Chem. Eng. J.*, **9**, 197 (1975).

Brenner, H., "The Diffusion Model of Longitudinal Mixing in Beds of Finite Length Numerical Values," *Chem. Eng. Sci.*, **17**, 229 (1962).

Carleton, A. J., R. J. Flain, J. Rennie, and F. H. H. Valentine, "Some Properties of Packed Bubble Columns," *Chem. Eng. Sci.*, **22**, 1839 (1967).

Danckwerts, P. V., *Gas-Liquid Reactions*, Ch. 5, McGraw Hill, New York (1970).

Deckwer, W. D., and A. Schumpe, "Bubble Columns—the State of the Art and Current Trends," *Int. Chem. Eng.*, **27**(3), 405 (1987).

Deckwer, W. D., R. Burckhart, and G. Zoll, "Mixing and Mass Transfer in Tall Bubble Column," *Chem. Eng. Sci.*, **29**, 2177 (1974).

Diboun, M., and K. Schugerl, "Eine Blasensaule Mit Gleichstrom Von Wasser Und Luft: I. Mischungsvorgange In Der Gasphase," *Chem. Eng. Sci.*, **22**, 147 (1967).

Field, R. W., and J. F. Davidson, "Axial Dispersion in Bubble Columns," *Trans. Inst. Chem. Engrs.*, **58**, 228 (1980).

Godbole, S. P., M. F. Honath, and Y. T. Shah, "Holdup Structure in Highly Viscous Newtonian and Non-Newtonian Liquids in Bubble Columns," *Chem. Eng. Commun.*, **16**, 119 (1982).

Godbole, S. P., S. Joseph, Y. T. Shah, and N. L. Carr, "Hydrodynamics of Mass Transfer in Bubble Columns with an Organic Liquid," *Can. J. Chem. Eng.*, **62**, 440 (1984a).

Godbole, S. P., A. Schumpe, Y. T. Shah, and N. L. Carr, "Hydrodynamics and Mass Transfer in Non-Newtonian Solutions in a Bubble Column," *AIChE J.*, **30**(2), 213 (1984b).

Heijnen, I., and K. Van't Riet, "Mass Transfer, Mixing and Heat Transfer Phenomena in Low-Viscosity Bubble-Column Reactors," *Chem. Eng. J.*, **28**, B21 (1984).

Hikita, H., S. Asai, K. Tanigawa, K. Segawa, and M. Kitao, "Gas Holdup in Bubble Columns," *Chem. Eng. J.*, **20**, 59 (1980).

Joseph, S., and Y. T. Shah, "Errors Caused by Tracer Solubility in the Measurement of Gas-Phase Dispersion," *Can. J. Chem. Eng.*, **64**, 122 (1986).

Joseph, S. Y. T. Shah, and B. G. Kelkar, "A Simple Experimental Technique to Measure Gas-Phase Dispersion in Bubble Columns," *Chem. Eng. Commun.*, **24**, 105 (1985).

Joseph, S., and Y. T. Shah, "A Two-Bubble-Class Model for Churn-Turbulent Bubble-Column Slurry Reactor," *ACS Symp. Ser.*, **27**, 149 (1984).

Joshi, J. B., "Gas-Phase Dispersion in Bubble Columns," *Chem. Eng. J.*, **24**, 213 (1982).

Joshi, J. B., "Axial Mixing in Multiphase Contactors—a Unified Correlation," *Trans. Inst. Chem. Engrs.*, **58**, 155 (1980).

Joshi, J. B., A. B. Pandit, and K. Raghav Rao, "Axial Mixing in Multiphase Sparged Contactors," *Encyclopedia of Fluid Mechanics*, Vol. 3, p. 1137, N. P. Cheremisinoff, ed., Gulf Publishing (1986).

Joshi, J. B., and M. M. Sharma, "A Circulation Cell Model for Bubble Columns," *Trans. Inst. Chem. Engrs.*, **57**(4), 244 (1979).

Kago, T., Y. Sasaki, T. Kondu, S. Morooka, and Y. Kato, "Gas

Holdup and Axial Dispersion in Bubble Columns of Homogeneous Flow Regime," *Chem. Eng. Commun.*, **75**, 23 (1989).

Kelkar, B. G., S. P. Godbole, M. F. Honath, Y. T. Shah, N. L. Carr, and W. D. Deckwer, "Effect of Addition of Alcohols on Gas Holdup and Backmixing in Bubble Columns," *AIChE J.*, **29** (3), 361 (1983).

Kolbel, H., H. Langemann, and J. Platz, *Dechema Monographien*, **41**, 225 (1962).

Kubo, K., K. Koya, and T. Miyauchi, "Operating Characteristics of Pulsed Gas Bubble Columns with Perforated Plates," *Kagaku Kogaku*, **34**, 856 (1970).

Kulkarni, A., and Y. T. Shah, "Gas-Phase Dispersion in a Downflow Bubble Column," *Chem. Eng. Commun.*, **28**, 311 (1984).

Levenspiel, O., *Chemical Reaction Engineering*, p. 253, Wiley Eastern Press, New York (1972).

Lubbert, A., private communication (1990).

Mangartz, K. H., and Th. Pilhofer, "Interpretation of Mass-Transfer Measurements in Bubble Columns Considering Dispersion of Both Phases," *Chem. Eng. Sci.*, **36**, 1969 (1981).

Men'shchikov, V. A., and M. E. Aerov, "Longitudinal Mixing of Gas Phase in Bubble-Plate Reactors," *Theo. Found. Chem. Eng.*, **1**, 739 (1967).

Mikio, K., and O. Tsutao, "Gas Phase Mixing In Bubble Columns," preprint German/Japanese Symp. on Bubble Columns (1988).

Molerus, O., and M. Kurtin, "Hydrodynamics of Bubble Columns in the Liquid Recirculation Regime," *Chem. Eng. Sci.*, **41**(10), 2685 (1986).

Nakanoh, M., and F. Yoshida, "Gas Absorption by Newtonian and Non-Newtonian Liquids in a Bubble Column," *Ind. Eng. Chem. Proc. Des. Dev.*, **19**, 190 (1980).

Nelder, J. A., and R. Mead, "Simplex Method for Function Minimization," *Comp. J.*, **7**, 308 (1965).

Patel, S. A., J. G. Daly, and D. B. Bukur, "Holdup and Interfacial Area Measurements Using Dynamic Gas Disengagement," *AIChE J.*, **35**(6), 931 (1989).

Press, W. H., B. P. Flannery, S. A. Teukolsky, and W. T. Vetterling, *Numerical Recipes: the Art of Scientific Computing*, Cambridge University Press (1986).

Radeke, K. H., "Critical Remarks on Using Moments Methods," *Ind. Eng. Chem. Fund.*, **20**, 302 (1981).

Schumpe, A., and W. D. Deckwer, "Gas Holdups, Specific Interfacial Areas and Mass-Transfer Coefficients of Aerated Carboxymethyl Cellulose Solutions in a Bubble Column," *Ind. Eng. Chem. Process Des. Dev.*, **21**, 706 (1982).

Schumpe, A., and G. Grund, "The Dynamic Gas Disengagement Technique for Studying Gas Holdup Structure in Bubble Columns," *Can. J. Chem. Eng.*, **64**, 891 (1986).

Seher, A., and V. Schumacher, "Gas-Phase Dispersion in Bubble Columns," *Ger. Chem. Eng.*, **2**, 117 (1979).

Shah, Y. T., B. G. Kelkar, S. P. Godbole, and W. D. Deckwer, "Design Parameters Estimation for Bubble Column Reactors," *AIChE J.*, **28**, 353 (1982).

Shah, Y. T., G. J. Steigel, and M. M. Sharma, "Backmixing in Gas-Liquid Reactors," *AIChE J.*, **24**(3), 369 (1978).

Shetty, S. A., "Gas-Phase Backmixing in Bubble Column Reactors," MS Thesis, Univ. of Tulsa (1991).

Sriram, K., and R. Mann, "Dynamic Gas Disengagement: a New Technique for Assessing the Behavior of Bubble Columns," *Chem. Eng. Sci.*, **32**, 571 (1977).

Stehfest, M., "Numerical Inversion of Laplace Transform," *Comm. ACM*, **13**(1), 47 (1970).

Towell, G. D., and G. H. Ackermann, "Axial Mixing of Liquid and Gas in Large-Bubble Reactors," *Euro./Int. Symp. Chem. Reaction Eng.*, B3-1, Elsenz, Amsterdam (1972).

Vanderlaan, Th., "Notes on the Diffusion Type Model for the Longitudinal Mixing in Flow," *Chem. Eng. Sci.*, **1**, 87 (1957).

Vermeer, D., and R. Krishna, "Hydrodynamics and Mass Transfer in Bubble Columns Operating in the Churn-Turbulent Regime," *Ind. Eng. Chem. Proc. Des. Dev.*, **20**, 475 (1981).

Wachi, S., and Y. Nojima, "Gas Phase Dispersion in Bubble Columns," *Chem. Eng. Sci.*, **45**(4), 901 (1990).

Manuscript received Mar. 22, 1991, and revision received Mar. 20, 1992.